Probing Inhibitor-Induced Conformational Changes along the Interface between Tissue Factor and Factor VIIa

Maria Österlund,[‡] Rikard Owenius,[§] Karin Carlsson,[‡] Uno Carlsson,[‡] Egon Persson,[||] Mikael Lindgren,[§,⊥] Per-Ola Freskgård,*[,#] and Magdalena Svensson*[,‡]

IFM-Department of Chemistry, Linköping University, Linköping, Sweden, IFM-Department of Chemical Physics, Linköping University, Linköping, Sweden, Vascular Biochemistry, Novo Nordisk A/S, Måløv, Denmark, and Protein Biotechnology, Novo Nordisk A/S, Bagsværd, Denmark

Received February 9, 2001; Revised Manuscript Received May 24, 2001

ABSTRACT: Upon injury of a blood vessel, activated factor VII (FVIIa) forms a high-affinity complex with its allosteric regulator, tissue factor (TF), and initiates blood clotting. Active site-inhibited factor VIIa (FVIIai) binds to TF with even higher affinity. We compared the interactions of FVIIai and FVIIa with soluble TF (sTF). Six residues in sTF were individually selected for mutagenesis and site-directed labeling. The residues are distributed along the extensive binding interface, and were chosen because they are known to interact with the different domains of FVIIa. Fluorescent and spin probes were attached to engineered Cys residues to monitor local changes in hydrophobicity, accessibility, and rigidity in the sTF−FVIIa complex upon occupation of the active site of FVIIa. The results show that inhibition of FVIIa caused the structures around the positions in sTF that interact with the protease domain of FVIIa to become more rigid and less accessible to solvent. Thus, the presence of an active site inhibitor renders the interface in this region less flexible and more compact, whereas the interface between sTF and the light chain of FVIIa is unaffected by active site occupancy.

Tissue factor (TF)[1] is a cell-surface transmembrane protein that initiates the blood coagulation cascade by acting as a cofactor for activated factor VII (FVIIa) (*1*). The extracellular part of TF (sTF) consists of two domains with fibronectin-type III topology, and it binds both FVIIa and FVII. FVIIa is composed of a protease domain (PD), two EGF-like domains (EGF1 and EGF2), and a γ-carboxyglutamic acid (Gla) domain. The four-domain structure of FVIIa and the two-domain structure of sTF form a tight complex with an extensive binding interface (*2*, *3*) that encompasses three binding regions, designated sTF−PD, sTF−EGF1, and sTF−Gla (Figure 1). The crystal structures of active site-inhibited FVIIa (FVIIai) alone (*4*) and in complex with sTF (*2*) have been determined, and the latter probably represents the structure of FVIIa in its most active form. Detailed comparison of the two structures reveals several structural differences. For example, the orientation of the active site inhibitor differs in free and sTF-bound FVIIa, suggesting a role for TF in substrate recognition. The crystal structure of FVIIa without the presence of an active site inhibitor has not yet been reported. Biochemical studies have demonstrated that incorporation of an inhibitor into the active site of FVIIa increases the affinity of binding to TF (*5*−*7*), probably by

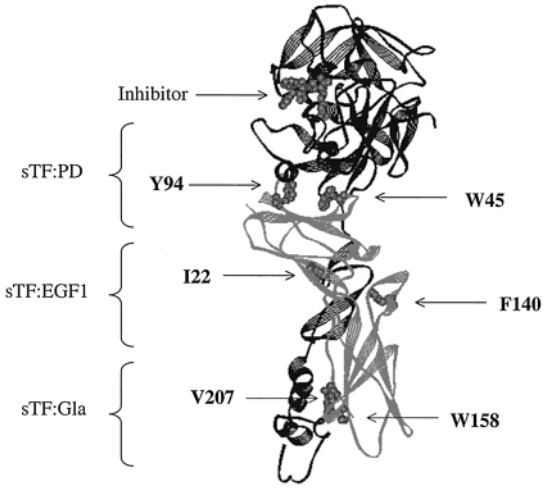

FIGURE 1: Structure of sTF (gray) in complex with FVIIai (black) (*2*) showing the different binding regions within the complex. The active site inhibitor in FVIIa and the six mutated and labeled positions in sTF are highlighted in gray ball-and-stick structures.

[†] M.Ö. and R.O. are Ph. D. students at the Graduate School Forum Scientum which is funded by the Swedish Foundation for Strategic Research. This work was also supported by grants from the Swedish Medical Research Council (U.C. and M.S.) and the Swedish Natural Science Research Council (U.C.).

* To whom correspondence should be addressed. M.S.: telephone, +46 13285686; fax, +46 13281399; e-mail, msv@ifm.liu.se. P.-O.F.: telephone, +45 44434356; fax, +45 44434417; e-mail, pof@novonordisk.com.

[‡] IFM-Department of Chemistry, Linköping University.

[§] IFM-Department of Chemical Physics, Linköping University.

[||] Vascular Biochemistry, Novo Nordisk A/S.

[⊥] Present address: Department of Laser Systems, Division of Sensor Technology, Swedish Defence Research Agency, P.O. Box 1165, SE-581 11 Linköping, Sweden.

[#] Protein Biotechnology, Novo Nordisk A/S.

[1] Abbreviations: sTF, soluble tissue factor; FVIIa, factor VIIa; FVIIai, inhibited FVIIa; PD, protease domain; EGF, epidermal growth factor-like domain; Gla, γ-carboxyglutamic acid; EPR, electron paramagnetic resonance; IAEDANS, 5-({[(2-iodoacetyl)amino]ethyl}-amino)naphthalene-1-sulfonic acid; IPSL, *N*-(1-oxyl-2,2,5,5-tetramethyl-3-pyrrolidinyl)iodoacetamide.

10.1021/bi010283n CCC: $20.00
Published on Web 07/12/2001

inducing conformational changes in the PD (*6*).

Our aim was to further investigate the conformational changes that occur in the extended interface between sTF and FVIIa upon inhibitor binding. For this purpose, we constructed two sTF mutants in each of the three binding regions. We used the site-directed labeling technique, which can provide structural information by introducing reporter groups such as fluorescent or spin-labels into the protein of interest (*8*, *9*). It involves introduction of a Cys residue at a desired position in the protein, followed by attachment of a sulfhydryl-specific spectroscopic label. Such labels are sensitive to their local environment and can therefore monitor changes that occur in the vicinity of the site of mutation. This methodology enabled us to specifically register inhibitor-induced conformational changes in one particular binding region of the interface between sTF and FVIIa.

MATERIALS AND METHODS

Chemicals. *N*-(1-Oxyl-2,2,5,5-tetramethyl-3-pyrrolidinyl)-iodoacetamide (IPSL) was purchased from Sigma (St. Louis, MO), and 5-({[(2-iodoacetyl)amino]ethyl}amino)naphthalene-1-sulfonic acid (IAEDANS) was from Molecular Probes (Eugene, OR). The chemicals that were used were analytical grade.

Spectrophotometers. Protein concentrations were determined on a Hitachi U-2000 spectrophotometer, and fluorescence measurements were performed on a Hitachi F-4500 instrument equipped with a thermostatic sample compartment unit with a magnetic stirrer.

Protein Purification and Labeling. The single-Cys mutants of sTF were produced, purified, and labeled as described previously (*10*). FVIIa was isolated and optionally modified with the active site inhibitor FFR-chloromethyl ketone (*6*, *11*, *12*).

Activity Measurements. An amidolytic assay was performed to determine the cofactor activity of the labeled sTF variants as described previously (*13*). Briefly, 10 nM FVIIa was titrated in separate experiments with the sTF variants (0−500 nM) in 50 mM Hepes, 150 mM NaCl, and 5 mM $CaCl_2$ (pH 7.5).

EPR Spectroscopy Measurements. Three different samples were prepared containing an IPSL-labeled sTF variant in 50 mM Hepes, 150 mM NaCl, and 5 mM $CaCl_2$ (pH 7.5): (1) sTF, (2) sTF−FVIIa, and (3) sTF−FVIIai. The concentration of the spin-labeled sTF variant was 4.0 μM, and the FVIIa/FVIIai concentration was 6.0 μM. Measurements were performed with both IPSL-labeled Y94C- and W45C-sTF. Each sample was introduced in a standard 400 μL TM_{110} flat cell for aqueous samples (Wilmad Glass, Buena, NJ). EPR measurements were carried out using a Bruker continuous wave X-band spectrometer (Bruker Analytik GmbH, Rheinstetten/Karlsruhe, Germany) consisting of a combination of the ER200D-SRC and ESP300 systems and an ER4103TM cavity connected to the 200 mW microwave bridge. The modulation amplitude was set lower than one-half of the line width of the $m_I = 0$ nitrogen hyperfine transition (1.2 G), and EPR spectra were recorded at a microwave power of 4 mW. All measurements were performed under equilibrium conditions at room temperature (21 ± 1 °C). All first-derivative EPR spectra were baseline-corrected and normalized to a constant spin concentration (Bruker Win-EPR 2.11 and Matlab 5.2).

Fluorescence Measurements. Samples were prepared consisting of protein in 5 mM $CaCl_2$, 50 mM Hepes, and 150 mM NaCl (pH 7.5). The IAEDANS molecule was excited at 350 nm while recording the fluorescence emission at 420−550 nm from three separate samples: free sTF, sTF−FVIIa, and sTF−FVIIai. Protein concentrations were 0.25 μM IAEDANS-labeled sTF variant and 0.5 μM FVIIa/FVIIai. The same samples were used for subsequent acrylamide quenching of the fluorescence. The IAEDANS fluorescence was quenched by progressive addition every 8 s of 2.5 μL aliquots of a 5.6 M acrylamide solution with continuous stirring. After excitation of the IAEDANS molecule, quenching was monitored at the emission maximum. Quenching data were analyzed according to the Stern−Volmer equation

$$\frac{F_0}{F} = 1 + K_{SV}[Q]$$

where F_0 is the total fluorescence in the absence of quencher, K_{SV} is the Stern−Volmer constant, and F is the measured fluorescence at a quencher concentration [Q]. K_{SV} values were calculated for each sample. All measurements were performed at 23 °C.

RESULTS AND DISCUSSION

Biochemical studies have shown that incorporation of an inhibitor into the active site of FVIIa increases the binding affinity between sTF and FVIIa (*5*−*7*). Since an extensive binding interface is formed during association of these two molecules (*2*, *3*), there are many regions where the interaction may be altered. So far, the increase in binding affinity between sTF and FVIIa upon incorporation of an inhibitor in the active site has been attributed to changes at the sTF−PD interface (*6*). However, Leonard et al. (*14*) recently found that conformational changes occur in the EGF1 domain in free FVIIa upon occupation of the active site by an inhibitor. We used site-directed labeling to incorporate spectroscopic probes along the entire binding interface between sTF and FVIIa. These probes were intended to serve as sensors to register any differences in the local environment in the absence or presence of an active site inhibitor in the sTF−FVIIa complex. We used two sTF residues in each of the three sTF−FVIIa binding regions: Y94 and W45 in the sTF−PD region, F140 and I22 in the sTF−EGF1 region, and W158 and V207 in the sTF−Gla region. These residues were individually replaced with Cys (Figure 1), and a fluorescent probe (IAEDANS) was attached to each of the engineered Cys residues in sTF. All six labeled variants retained reasonable affinity for FVIIa and were able to stimulate its amidolytic activity. The following results were obtained [equilibrium dissociation constant (7 nM for wt-sTF) and activity (compared to that of wt-sTF which was set to 100%)] in a previously described functional assay (*13*, *15*): Y94C-IAEDANS, 130 nM and 33%; W45C-IAEDANS, 230 nM and 31%; F140C-IAEDANS, 40 nM and 86%; I22C-IAEDANS, 66 nM and 104%; W158C-IAEDANS, 10 nM and 88%; and V207C-IAEDANS, 13 nM and 82%, respectively. The complexes containing sTF variants with mutations in positions contacting the light chain of FVIIa appeared to have normal activity, whereas the two first variants, with mutations in positions contacting the PD in FVIIa, exhibited

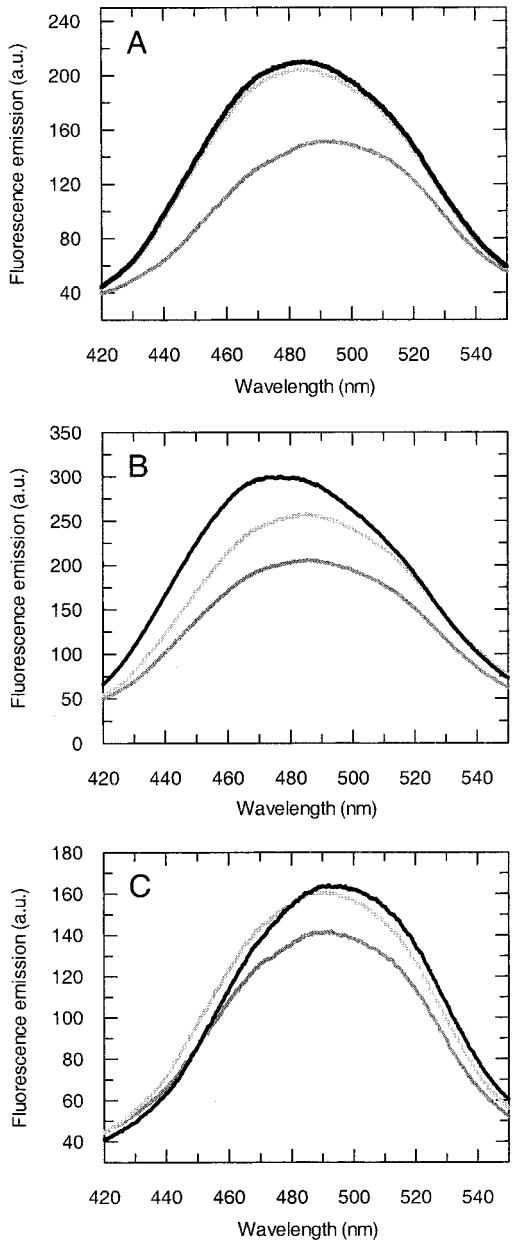

FIGURE 2: Fluorescence emission spectra of the IAEDANS-labeled sTF variants. The labeled positions were F140C (A), W45C (B), and Y94C (C), and the figures show spectra of sTF (gray; bottom curve), the sTF−FVIIa complex (light gray; middle curve), and the sTF−FVIIai complex (black; top curve).

an impaired cofactor activity. However, in these two cases, the activity enhancement on complex formation was still almost 10-fold, indicating that the native complex is formed and that the Cys-IAEDANS residue cannot functionally replace the wild-type residue in these two positions. The data justify the use of the sTF variants in characterizing the effects of an active site inhibitor on the sTF−FVIIa complex. Fluorescence emission spectra were recorded for free sTF and for sTF in complex with FVIIa or FVIIai. Results of the fluorescence measurements at one representative position, IAEDANS-labeled position 140 at the border of the sTF−EGF1 and sTF−Gla regions, are shown in Figure 2A. No difference in polarity between the sTF−FVIIa and sTF−FVIIai complexes was sensed by the fluorophore in this position according to the emission wavelength maximum. Exactly the same behavior was observed for positions 22, 140, 158, and 207 (data not shown). This clearly suggests that neither the sTF−EGF1 nor the sTF−Gla binding interface is affected by occupancy of the active site of FVIIa. This does not support the hypothesis of Leonard and coworkers that conformational changes occur in the sTF−EGF1 region upon inhibitor binding (*14*). However, that assumption was based on data from measurements on free FVIIa, using a monoclonal antibody that specifically binds to residues 51−88 in EGF1. The inhibitor-induced conformational changes detected in EGF1 of free FVIIa may reflect conformational changes occurring in the PD but being sensed by other domains due to interdomain contacts in the potentially compact structure of free FVIIa (*16*). On the contrary, during our measurements, an elongated shape of FVIIa is ensured by the binding to sTF.

The fluorescence spectrum of sTF labeled at position 45 in complex with FVIIa shows a significant blue shift upon addition of inhibitor, which indicates that the environment around the probe has become more apolar (Figure 2B). In contrast, corresponding measurements at position 94 show a red shift (Figure 2C). Thus, the fluorescence emission maxima for the two sTF−FVIIai complexes demonstrate a difference in polarity between the two positions.

Since no effects of active site occupancy on the fluorescence emission could be detected at any of the other sTF positions in the binding interface of the sTF−FVIIa complex, we continued our study solely on the two specific sites in the sTF−PD interface, W45 and Y94 in sTF. According to Banner et al. (*2*), five key interactions occur in the sTF−PD binding interface, two of which involve W45 and Y94. W45 appears to be necessary for the affinity (*17*), whereas Y94 is presumably more important for the allosteric activation of FVIIa (*18*). A spin-label, IPSL, was attached to an engineered Cys residue at these positions to serve as a sensor for the binding between sTF and FVIIa/FVIIai. The spin-labeled sTF variants, Y94C-IPSL and W45C-IPSL, had affinities for FVIIa described by dissociation constants of 99 and 1600 nM, respectively, and the complexes with FVIIa had amidolytic activities that were 57 and 85%, respectively, of that of the wild-type complex. EPR spectra of free spin-labeled sTF as well as spin-labeled sTF in complex with FVIIa/FVIIai are presented in Figure 3. The line shape of the spectrum is influenced by the mobility of the spin-label, which can be restricted by the surrounding groups. The less mobile the spin-label, the greater the contribution of the anisotropic hyperfine interaction, which results in a broadening of the spectral bands. Complex formation between sTF and FVIIa or FVIIai places motional restrictions on IPSL. Thus, from the spectra, it is apparent that the spin-label is less mobile in the sTF−FVIIai than in the sTF−FVIIa complex. The relatively low dissociation constant for Y94C-IPSL ensures that close to 100% of the sTF molecules are included in the complex. Thus, the spectral broadening must be due to a more rigid immediate environment of IPSL at position 94 when an active site inhibitor is present. Two-component line-shape simulations showed a major increase of the slow-mobility component upon addition of the inhibitor (from 26 to 54%), further corroborating the above conclusion (data not shown). The situation is somewhat complicated by the high dissocitaion constant for W45C-IPSL, causing a fraction of the sTF molecules (22%) to be uncomplexed. However, addition of FVIIa leads to a

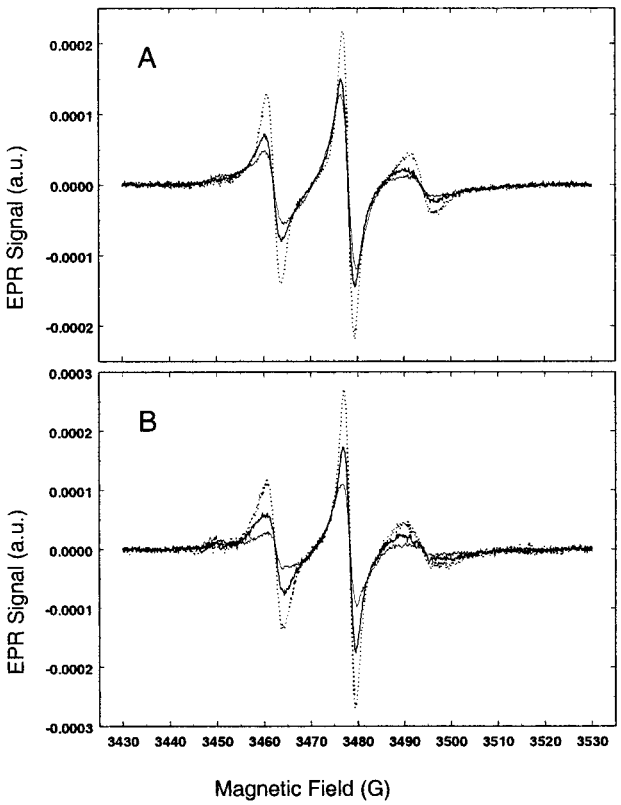

FIGURE 3: EPR spectra of IPSL-labeled sTF variants. The sTF mutants that were used were W45C (A) and Y94C (B), and the figures show spectra of sTF (•••), the sTF−FVIIa complex (gray), and the sTF−FVIIai complex (black).

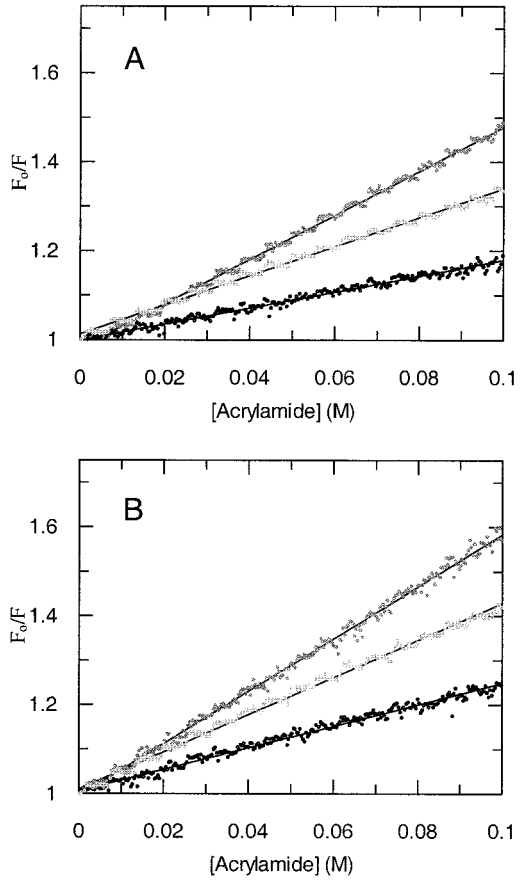

FIGURE 4: Stern−Volmer plots of the extent of acrylamide quenching of IAEDANS-labeled sTF variants. The mutants that were used were W45C (A) and Y94C (B), and the figures show the fluorescence of sTF (gray; top curve), the sTF−FVIIa complex (light gray; middle curve), and the sTF−FVIIai complex (black; bottom curve).

significant line broadening of the EPR spectrum, which is further broadened by binding of the active site inhibitor. Altogether, this demonstrates that the vicinal structure of the probes becomes more rigid and compact in the presence of an active site inhibitor. This agrees with earlier studies showing that active site occupancy of FVIIa results in tighter binding of sTF (*5*−*7*). Previous results concerning position 94 are ambiguous. Kelley et al. (*19*) have reported that this position makes a major contribution to the binding energy ($\Delta\Delta G$ = 1 kcal/mol), whereas Ruf and co-workers have found only insignificant involvement of Y94 (*17*). Nevertheless, our observations demonstrate that positions 45 and 94 are both affected by the presence of an active site inhibitor.

We also probed the complex formation by studying the accessibility of the fluorescent labels at positions 45 and 94 in sTF. The IAEDANS fluorescence was progressively quenched by adding acrylamide to the protein solution. Acrylamide quenching of IAEDANS-labeled sTF alone and in complex with either FVIIa or FVIIai is illustrated in Figure 4. The extent of quenching was different (sTF > TF−FVIIa > sTF−FVIIai), indicating that attachment of an inhibitor reduces the accessibility of the labeled site. A more thorough comparison of the two positions showed that the label at position 45 loses much of its accessibility already upon binding of FVIIa (K_{SV} decreased from 5.0 to 2.4 M^{-1}) but becomes only slightly more buried upon inhibitor binding to the active site of FVIIa (K_{SV} = 1.8 M^{-1}). In contrast, the accessibility of position 94 is moderately decreased upon complex formation with FVIIa (K_{SV} decreased from 5.9 to 4.2 M^{-1}) but is significantly further decreased in the sTF−FVIIai complex (K_{SV} = 2.4 M^{-1}). Thus, introduction of an inhibitor in FVIIa has a large effect on the label in position 94. This is in agreement with studies on FVIIa where mutations of Met306, which in the FVIIa−sTF complex is wedged in a hydrophobic groove formed in part by Tyr94, abolish or reduce the effect of active site occupancy on the affinity of FVIIa for sTF (*7*, *20*). Additionally, since EPR and quenching data implied a rigid structure and inaccessible location of the labeled site in position 94, we suggest that the observed red shift in the fluorescence measurements originates from a closer contact of this region with polar residues Gln308 and Asp309 (*2*) in FVIIa upon the incorporation of an inhibitor.

In conclusion, our results show that the active site inhibitor makes the sTF−FVIIa complex more stable and more compact in the regions around both Trp45 and Tyr94 in the sTF−PD interface, whereas the sTF−EGF1 and sTF−Gla interfaces are unaffected.

REFERENCES

1. McVey, J. H. (1999) *Bailliere's Best Practice in Clinical Haematology 12*, 361−372.
2. Banner, D. W., D'Arcy, A., Chene, C., Winkler, F. K., Guha, A., Konigsberg, W. H., Nemerson, Y., and Kirchhofer, D. (1996) *Nature 380*, 41−46.
3. Zhang, E., St. Charles, R., and Tulinsky, A. (1999) *J. Mol. Biol. 285*, 2089−2104.
4. Pike, A. C., Brzozowski, A. M., Roberts, S. M., Olsen, O. H., and Persson, E. (1999) *Proc. Natl. Acad. Sci. U.S.A. 96*, 8925−8930.

5. Higashi, S., Matsumoto, N., and Iwanaga, S. (1996) *J. Biol. Chem. 271*, 26569−26574.
6. Sørensen, B. B., Persson, E., Freskgård, P. O., Kjalke, M., Ezban, M., Williams, T., and Rao, L. V. (1997) *J. Biol. Chem. 272*, 11863−11868.
7. Dickinson, C. D., and Ruf, W. (1997) *J. Biol. Chem. 272*, 19875−19879.
8. Carlsson, U., and Jonsson, B. H. (1995) *Curr. Opin. Struct. Biol. 5*, 482−487.
9. Hubbell, W. L., Gross, A., Langen, R., and Lietzow, M. A. (1998) *Curr. Opin. Struct. Biol. 8*, 649−656.
10. Owenius, R., Österlund, M., Lindgren, M., Svensson, M., Olsen, O. H., Persson, E., Freskgård, P. O., and Carlsson, U. (1999) *Biophys. J. 77*, 2237−2250.
11. Thim, L., Bjoern, S., Christensen, M., Nicolaisen, E. M., Lund-Hansen, T., Pedersen, A. H., and Hedner, U. (1988) *Biochemistry 27*, 7785−7793.
12. Freskgård, P. O., Olsen, O. H., and Persson, E. (1996) *Protein Sci. 5*, 1531−1540.
13. Persson, E., Olsen, O. H., Østergaard, A., and Nielsen, L. S. (1997) *J. Biol. Chem. 272*, 19919−19924.
14. Leonard, B. J. N., Clarke, B. J., Sridhara, S., Kelley, R., Ofosu, F. A., and Blajchman, M. A. (2000) *J. Biol. Chem. 275*, 34894−34900.
15. Österlund, M., Owenius, R., Persson, E., Lindgren, M., Carlsson, U., Freskgård, P. O., and Svensson, M. (2000) *Eur. J. Biochem. 267*, 6204−6211.
16. Freskgård, P. O., Petersen, L. C., Gabriel, D. A., Li, X., and Persson, E. (1998) *Biochemistry 37*, 7203−7212.
17. Ruf, W., Kelly, C. R., Schullek, J. R., Martin, D. M., Polikarpov, I., Boys, C. W., Tuddenham, E. G., and Edgington, T. S. (1995) *Biochemistry 34*, 6310−6315.
18. Dickinson, C. D., Kelly, C. R., and Ruf, W. (1996) *Proc. Natl. Acad. Sci. U.S.A. 93*, 14379−14384.
19. Kelley, R. F., Costas, K. E., O'Connell, M. P., and Lazarus, R. A. (1995) *Biochemistry 34*, 10383−10392.
20. Persson, E., Nielsen, L. S., and Olsen, O. H. (2001) *Biochemistry 40*, 3251−3256.

BI010283N